

Aligned explanations in neural networks

Corentin Lobet ^{1,✉}

Francesca Chiaromonte ^{1,2}

¹ Institute of Economics and L'EMBEDS, Sant'Anna School of Advanced Studies - Italy

² Dept. of Statistics and Huck Institutes of the Life Sciences, Penn State University - USA

✉ corentin.lobet@santannapisa.it

 [Paper Code](#)

Abstract

Feature attribution is the dominant paradigm for explaining the predictions of complex machine learning models like neural networks. However, most existing methods offer little guarantee of reflecting the model's prediction-making process. We define the notion of explanatory alignment and argue that it is central to trustworthy predictive modeling: in short, it requires that explanations directly underlie predictions rather than serve as rationalizations. We present model readability as a design principle enabling alignment, and Pointwise-interpretable Networks (PiNets) as a modeling framework to pursue it in a deep learning context. PiNets combine statistical intelligence with a pseudo-linear structure that yields instance-wise linear predictions in an arbitrary feature space. We illustrate their use on image classification and segmentation tasks, demonstrating that PiNets produce explanations that are not only aligned by design but also faithful across other dimensions: meaningfulness, robustness, and sufficiency.

Field Keywords: Deep Learning, xAI, Feature Attribution, Saliency, Segmentation, Faithfulness

Novel Keywords: Explanatory Alignment, Readability, Pseudo-linear model, PiNet

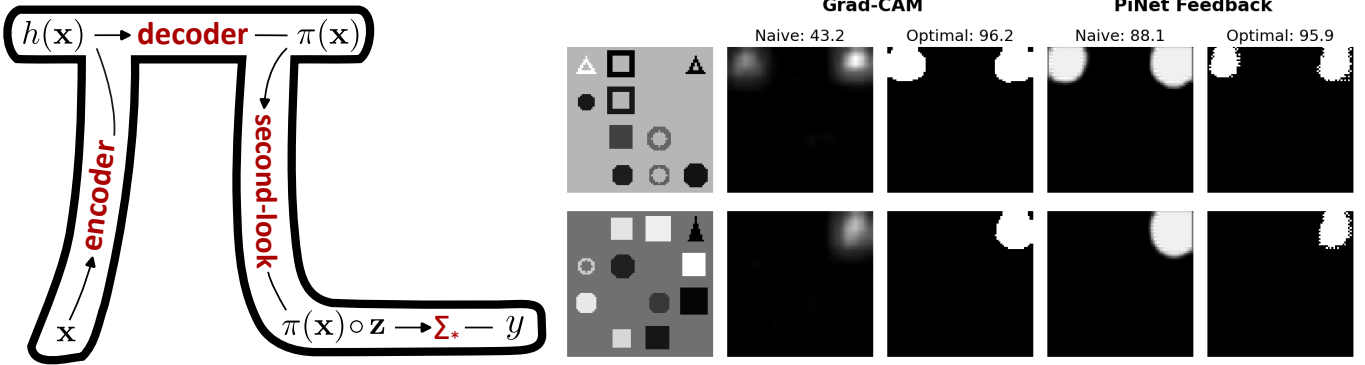


Figure 1: Generic architecture of a PiNet (**left**) and examples of Grad-CAM and PiNet explanations (attribution maps) in the ToyShapes task (**right**); column headings specify the post-processing approach (naive or optimal) and the test detection score (defined in eq. (11)).

1 Growing out of white-painting

White-painting The trust we place in a decision depends on the quality of its justification. When a decision is justified by a post-hoc rationalization or an ambiguous explanation, its trustworthiness is compromised; the justification is not fully **aligned** with the actual decision-making

process. While such limitations are known to occur in human cognition [1–3], it should be a priority to circumvent them when automating decisions [4, 5]. One might further argue that it is precisely because we, humans, fall short on this front that improving transparency in the



making of AI-driven decisions is crucial.

Feature attribution is a major paradigm in the explainable artificial intelligence (xAI) literature [6–9]; a model’s prediction is explained by attributing importance scores to a predefined feature set (e.g., input features). Formally, for a prediction $y \in \mathcal{Y}$ constructed from input features $\mathbf{x} \in \mathcal{X}$ by a model $f : \mathcal{X} \rightarrow \mathcal{Y}$, we aim to generate an explanation $\hat{\pi} \in \mathcal{Z}$ that attributes scores to a set of features $\mathbf{z} \in \mathcal{Z}$.¹ In many cases, \mathcal{Z} coincides with the input space \mathcal{X} but this is not a requirement.

In spite of their significance in the scientific literature, feature attribution techniques usually fail to offer operational guarantees on their ability to achieve their intended purpose: *explaining how predictions are constructed by the model*. In this regard, they risk overstating their ability to “open the black-box” when in fact they may be painting it in white.

Sources of misalignment So-called black-box or model-agnostic explanation techniques [10–14] attempt to recover the model’s attributions π without direct access to the model’s inner workings. Typically, the explanation for some prediction $y = f(\mathbf{x})$ is estimated post-hoc by querying the model in the vicinity of the input \mathbf{x} ; the set of pairs (\mathbf{z}, y) thereby collected is used to form an estimate $\hat{\pi}$ of the model’s attributions π . Notably, SHAP and LIME [10, 11] belong to this family. Although the model-agnostic nature of such methods is appealing, they can fall short in terms of trustworthiness. For example, if \mathbf{z} is multicollinear a model-agnostic algorithm is faced with multiple ways to distribute importance across the feature set — i.e., multiple $\hat{\pi}$ — although only one corresponds to the model’s true attributions π . While, in theory, enough local perturbations of the data may help form a good approximation $\hat{\pi}$, of π the associated computational cost deepens the gap between theory and practice [15].

We note further that the very existence of attributions $\pi \in \mathcal{Z}$ made by the model is not guaranteed. In fact, the model may not even be designed to produce attributions π in the first place, and thus any $\hat{\pi}$ is necessarily a rationalization.

The safest approach to overcoming this risk of estimation error is to construct **intrinsic** explanations that, by construction, describe the prediction-making process and therefore cannot be mere rationalizations. But a vague intrinsicness condition is not sufficient to guard against misaligned explanations. We raise two caveats regarding *by-design* approaches that propose to design *inherently explainable* models. First, while such models indeed construct predictions and attributions within a shared pipeline, the intrinsic attributions π may not be produced prior to predictions y and thus act, at best, as parallel rationalizations of the latter [16]. The aforementioned shortcomings of post-hoc methods are then just transferred into the model. Second, when attributions do precede predictions within the model, making the two genuinely related, their relationship may remain difficult to grasp due to their computational distance [17–21]. That

is, the intrinsic function $g : \mathcal{Z}^2 \rightarrow \mathcal{Y}$ linking π and \mathbf{z} to the prediction y can be complex such that the interpretation of π as feature attributions is not straightforward.

To avoid these caveats, we shall prefer approaches that impose a strict condition of **immediate precedence** on how explanations relate to predictions. Explanations must be produced prior to predictions and be used directly to construct predictions via simple, interpretable operations. In particular, a single linear operation combining intrinsic attributions π with features \mathbf{z} is an optimal candidate as it makes the interpretation of explanations straightforward.

This idea, however, looks unhelpful given that it seems to imply working with the class of (generalized) linear models. As will be argued in this paper this turns out to be incorrect and there are, in fact, two ways to make this possible in neural networks. The dominant approach comes down to letting \mathbf{z} be the internal features learned by the neural network in its last layer. These internal features, sometimes called embeddings or rich encodings, are typically combined linearly to produce the output predictions, in which case the linear coefficients π (in this case, the weight parameters of the last layer) act as attributions and satisfy immediate precedence. In spite of that, the informational richness embedded in the internal features comes at the cost of their interpretability.

Concept-based learning aims to bridge this gap by fostering the construction of more interpretable internal features or labeling them once the model is trained [22–24]. Although promising, these methods are marked by subjective and inconsistent feature-labeling techniques [25, 26]. In response to these shortcomings it should be added that aligned explanations must be **fully interpretable**; that is, all features in the space \mathcal{Z} (in which attributions are formed) must be unambiguous.

The second way to obtain linear coefficients in neural networks is to design them as pseudo-linear models. This is the approach we pursue in this paper.

Before doing so, we must mention the peculiar case of gradient-based attributions [27–29]. Techniques in this category construct post-hoc explanations but do so with a direct access to the gradients of the model. Gradients (i.e., partial derivatives) are peculiar in that even though they are interpretable and intrinsic to the model, they are not produced prior to predictions and their interpretation as feature attributions is ambiguous [30–32]. Yet, and notably in image data, gradient-based methods can yield high-quality explanations that capture meaningful signals in the data; that is why we use one of those methods (Grad-CAMs) as baseline in the validation of our approach.

Contributions The philosophy defended in this paper can be summed up in the following motto: *let the model speak but make it speak clearly*. Explanations ought to be provided by the prediction model itself (intrinsic), directly underlie predictions (immediate precedence), and be communicated unambiguously (fully interpretable).

¹To reduce notational burden we assume $\hat{\pi} \in \mathcal{Z} \subseteq \mathbb{R}^D$ throughout the paper, although the scores need only lie in a space of dimension D such that the element-wise product $\hat{\pi} \circ \mathbf{z}$ lies in \mathbb{R}^D .



Toward this vision we start in Section 2 by defining explanatory alignment and presenting the notion of model readability as an operational design principle toward our goal. We then define the class of pseudo-linear models and identify it as a natural candidate to achieve readability in neural networks. Nonetheless, while the explanations produced by such models are aligned by design they may fall short in other aspects of faithfulness. We especially define and consider meaningfulness, robustness, and sufficiency and integrate them with alignment into a novel evaluation framework which we refer to as MARS.

In Section 3 we present the PiNets modeling framework alongside several training techniques for the design of readable networks delivering high predictive accuracy and explanatory faithfulness across the MARS criteria.

In Section 4 we validate our approach on image data, where explanations consist of detecting relevant pixels. In image classification, PiNets achieve performance comparable to Grad-CAMs [28] while producing aligned explanations and without compromising predictive accuracy. Moreover, PiNets can effortlessly be exposed to even a limited amount of ground-truth attributions during training to boost the quality of their explanations. Next, we use a semantic segmentation problem on satellite imagery to illustrate how the quality of PiNets' explanations can be improved when more informative target variables are available.

The discussion in Section 5 provides a more detailed summary of the paper and outlines directions for future research.

2 Grounding models in readability

Model readability Now that we have set the stage by listing some desired properties of explanations — intrinsicness, immediate precedence, and interpretability — we can define what an aligned explanation is.

Definition 1. Aligned explanation

Explanatory alignment at point $(\mathbf{x} \in \mathcal{X}, \mathbf{z} \in \mathcal{Z}, y = f(\mathbf{x}))$, is possible if \mathbf{z} is fully interpretable and the model f embeds both a feature attribution $\boldsymbol{\pi} \in \mathcal{Z}$ and a simple function $g : \mathcal{Z}^2 \rightarrow \mathcal{Y}$ such that $y = g(\boldsymbol{\pi}, \mathbf{z})$. Then, the attribution $\hat{\boldsymbol{\pi}} = \boldsymbol{\pi}$ is the perfectly aligned explanation.

The definition above and the three underlying properties lead to a structure-based answer: it is the functional form of the model that must be tweaked to achieve alignment. If we conceptualize model design as a two-stage process — a modeling stage followed by a training stage — alignment must be sought in the modeling stage. Furthermore, while the semantic quality of feature attributions can be a side effect of predictive accuracy and thus emerge during training [33, 34], alignment is not directly related to predictive performance.

We propose readability as a design principle on the model's structure to achieve alignment.

Definition 2. Readable model

A model $f : \mathcal{X} \rightarrow \mathcal{Y}$ producing predictions $y = f(\mathbf{x})$ is deemed readable if it can be rewritten in the form $y = g(\boldsymbol{\pi}, \mathbf{z})$, where $\mathbf{z} \in \mathcal{Z}$ is fully interpretable and $g : \mathcal{Z}^2 \rightarrow \mathcal{Y}$ is a simple aggregation function.

Under this structural constraint, reading the model effectively conveys how it combines the features \mathbf{z} to construct the prediction y . Together, the interpretability of features \mathbf{z} and the immediate precedence of explanations over predictions enforced by the readable function $g : \mathcal{Z}^2 \rightarrow \mathcal{Y}$, guarantee explanatory alignment.

Let us consider some classic examples. Linear models produce predictions by combining input features \mathbf{x} through a linear function $f(\mathbf{x}) = \sum_d \pi_d \cdot x_d$. If we produce explanations in the input space \mathcal{X} (i.e., $\mathcal{Z} \equiv \mathcal{X}$) it naturally follows that $g(\boldsymbol{\pi}, \mathbf{z}) = f(\mathbf{x})$, hence we have a highly interpretable functional form. Nevertheless, readability (and thus alignment) may be hindered by a high-dimensional or complex feature space [4] — oftentimes necessary to achieve reasonable levels of predictive accuracy. Similar considerations apply for generalized linear models (e.g., y can be a logit).

In contrast, decision trees typically partition a parsimonious feature space as they internally learn non-linearities and interactions [35]. However, it is usually their functional form (the tree) that grows in complexity to better fit the data. Consequently, the readability and alignment of tree-based models — whether deep individual trees or ensembles such as random forests [36] — may be compromised by their complex structure.

Interestingly, judicious integrations of linear and tree-based models can improve readability while offering reasonable predictive accuracy. For example, the RuleFit algorithm [37] estimates a linear model (simple g) over decision rules learned by tree-based models (interpretable \mathbf{z}).

Readable networks Where do deep neural networks fall on the readability spectrum? At first glance, they exhibit a complex functional form, especially as they become deeper. However, neural networks can also be read through the lens of their final layer. The construction of a prediction $y \in \mathcal{Y}$ can be written linearly as:

$$y = a + \sum_d \pi_d \cdot h_d(\mathbf{x}) \quad (1)$$

where $\mathbf{h} : \mathcal{X} \rightarrow \mathcal{Z}$ is an encoder producing rich features $\mathbf{h}(\mathbf{x})$ (used as \mathbf{z}). From this perspective, neural networks linearly combine internal features, and their lack of readability stems from these features rather than from their functional form. If the features $\mathbf{h}(\mathbf{x})$ were inter-



pretable, the model would be readable and the aligned explanation π would be accessible. As discussed in Section 1, concept-based learning methods seek to do exactly this but suffer from subjectivity in the labeling of features.

An alternative route consists in choosing which features to combine linearly in the last layer; that is, to use raw or handcrafted features $\mathbf{z} \in \mathcal{Z}$ rather than learned features $\mathbf{h}(\mathbf{x})$. To prevent the model from collapsing into a truly-linear form, we can embed complexity within the model’s coefficients: $\pi \equiv \pi(\mathbf{x})$. Such models belong to the class of varying-coefficient models (VCMs [8, 38, 39]) and we call **pseudo-linear models** their linear subclass wherein $\pi : \mathcal{X} \rightarrow \mathcal{Z}$ is a varying-coefficient function mapping the input features \mathbf{x} into coefficients that lie in the user-defined feature space \mathcal{Z} and where both are combined linearly to construct y .

Definition 3. Pseudo-linear model

Let \sum_* and \circ denote, respectively, element-wise summation and multiplication, and let us consider the two observable feature sets $\mathbf{x} \in \mathcal{X}$ and $\mathbf{z} \in \mathcal{Z}$ (we can have $\mathcal{X} \equiv \mathcal{Z}$). A pseudo-linear model takes the form:

$$y = a + \sum_* \pi(\mathbf{x}) \circ \mathbf{z} \quad (2)$$

Pseudo-linear models are linearly readable by design as long as \mathcal{Z} is fully interpretable. Such models effectively construct linear models instance-wise, i.e., any input $\mathbf{x} \in \mathcal{X}$ gives rise to a set of linear coefficients $\pi(\mathbf{x})$ then used to build the prediction $y = g(\pi, \mathbf{z})$ with g a linear aggregator.

Pseudo-linear networks The core idea behind pseudo-linear networks is to let $\pi(\mathbf{x})$ be a neural network, and the core mechanism that makes them readable is what we refer to as the **second look**. The coefficient set $\pi(\mathbf{x}) \in \mathcal{Z}$ is multiplied element-wise by the feature set $\mathbf{z} \in \mathcal{Z}$. We thus explicitly ask the model to look again at the data (through \mathcal{Z}) after extracting information from it (through \mathcal{X}). When $\mathcal{X} \equiv \mathcal{Z}$, the model examines the same information twice, yet in distinct ways. In both cases, the second look forces the model to learn rich coefficients $\pi(\mathbf{x})$ rather than rich features $\mathbf{h}(\mathbf{x})$.

Importantly, the second look must be seen as a mechanistic operation enabling immediate precedence, that is, it must be explicitly performed in the last layer of the network. For example, while B-cos networks [20] can be rewritten in a pseudo-linear form (at least when $\mathcal{Z} \equiv \mathcal{X}$) they do not rely on a second look in the last layer and do not satisfy immediate precedence.²

However, although it can enable readability, the second look is not sufficient to obtain explanations that capture meaningful signals in the data, especially in complex data structures. A notable attempt to design pseudo-linear networks is SENNs [40]. When working with image data the authors combined varying coefficients with learned concepts, i.e. $\mathbf{z} \equiv \mathbf{h}(\mathbf{x})$. As discussed previously,

this approach runs the risk of breaking alignment due to inconsistencies in feature labeling. More subtly, if we were convinced to learn unambiguous concepts the model would then be readable and aligned by design; and thus the recourse to varying coefficients in addition to concepts would be unnecessary, if not questionable.

In this paper, we tackle the challenge of designing readable networks without learning concepts, thereby maintaining control over the feature space \mathcal{Z} based on which explanations are formed. In doing so, the challenge no longer lies in producing aligned explanations — now a built-in property — but rather in achieving strong performance across other important dimensions of faithfulness, that we define below.

Faithfulness We introduce three additional evaluation criteria, each capturing a different aspect of explanatory faithfulness that we deem important alongside alignment. We integrate them into a novel evaluation framework (MARS) under which an explanation is faithful if:

- M Meaningful** - it captures the relevant signal;
- A Aligned** - it reflects the making of the prediction;
- R Robust** - it is not sensitive to context;
- S Sufficient** - it suffices to recover the prediction.

As an illustrative example, consider the classification of an input image picturing a cat and a litter box. We assume that the correct class prediction is $\tilde{y} = \text{“cat”}$, with \tilde{y} derived from the predicted logit $y \in \mathbb{R}$. We assume $\mathcal{X} \equiv \mathcal{Z}$, i.e. explanations $\hat{\pi}$ are formed or estimated in the input space \mathcal{X} .

We use the term “meaningfulness” to designate the accuracy of explanations with respect to ground truth attributions π^* . **Meaningfulness** reflects the ability of an explanation to capture and convey relevant signals in the data, such as an underlying causal structure or semantically pertinent features. Assuming an optimal explanation π^* exists, a perfectly meaningful explanation satisfies $\hat{\pi} = \pi^*$. In our example, this requires detecting the pixels that shape the cat (Figure 2 (M) top). Conversely, a failure to filter out spurious signal compromises meaningfulness: although the litter box may be statistically associated with the presence of a cat, it is spurious and should be disregarded (Figure 2 (M) bottom). Then, typically, hand-annotated segmentations of the cat can serve as ground-truth attributions to evaluate the meaningfulness of explanations.

Sufficiency requires that an explanation contain enough information to reconstruct the prediction [41, 42]. If it retains too little relevant signal or too much irrelevant signal, the explanation $\hat{\pi}$ can become misleading. Then, when the filtered signal, i.e. the element-wise product $\hat{\pi} \circ \mathbf{z}$, is used as input for a **recursive prediction** ($f(\hat{\pi} \circ \mathbf{z})$) the outcome may differ from the initial prediction ($f(\mathbf{x})$). In our example, detecting the cat’s tail only may not be sufficient to reliably infer that the image contains a cat if asked to predict from this detection (Figure 2 (S) bottom).

²The second look really occurs in the first layer and the pseudo-linear form appears once we rewrite the model formula to collapse every subsequent layer into one function. Their approach further requires $\mathcal{Z} \equiv \mathcal{X}$.



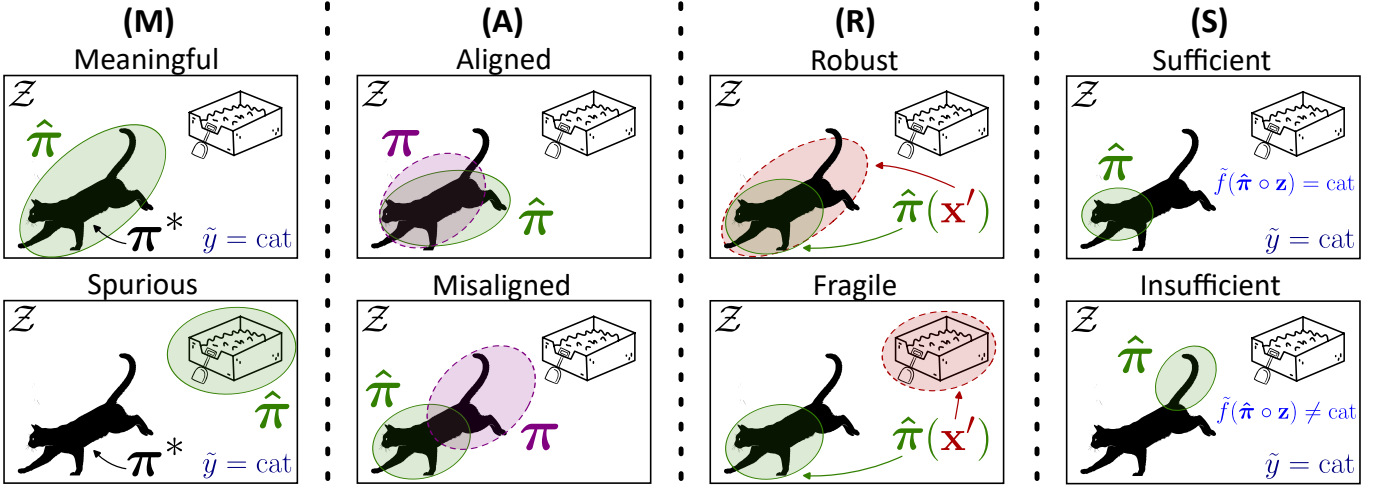


Figure 2: MARS criteria. An explanation is meaningful if it explains the prediction with relevant signal, aligned if it directly underlies the prediction, robust if it does not heavily rely on context, and sufficient if the prediction can be recovered from it.

Note that a sufficient explanation is not always meaningful, e.g., the cat’s head alone may suffice to correctly predict its presence so that the rest of the body can be disregarded (Figure 2 (S) top). Similarly, a meaningful explanation can be insufficient if explanations are misaligned. For example, assume we are given an explanation $\hat{\pi}$ capturing one half of the cat’s body whereas the model really uses the other half (π) to infer the presence of a cat (as in Figure 2 (A) bottom). Taking $\hat{\pi} \circ \mathbf{z}$ as recursive input — the wrong half of the cat — could then be insufficient to infer the cat’s presence as done initially.

We introduce the notion of robustness to context to extend the classic problem of reliance on spurious signal [43–45] to the field of xAI. **Robustness** requires that an explanation not rely heavily on contextual signal; that is, on cues that ought to be filtered out. Robustness can be compromised when explanations are not fixed but functions of the data, which naturally occurs in pseudo-linear models (that build $\pi(\mathbf{x})$) but can also be true with other approaches.³

Let \mathbf{x}' be the feature subset of \mathbf{x} that the *explainer*

(model or post-hoc technique) relies on to form the explanation, i.e., $\hat{\pi}(\mathbf{x}) = \hat{\pi}(\mathbf{x}')$. Then, if the explanation $\hat{\pi}(\mathbf{x}')$ assigns values close to zero to a substantial part of \mathbf{x}' , this part will be obscured in the recursive input $\hat{\pi}(\mathbf{x}) \circ \mathbf{x}$ (assuming $\mathbf{z} \equiv \mathbf{x}$). The recursive explanation built from it will then differ from the initial explanation because the model is now deprived of the signal used to build it, i.e. \mathbf{x}' . In our example, the initial explanation may highlight the cat ($\hat{\pi}(\mathbf{x}')$) yet rely on the litter box (\mathbf{x}') to do so. The box will subsequently be masked from the recursive input and thus cannot be used to build the recursive explanation (Figure 2 (R) top).

It is therefore preferable that the explainer ignores spurious contextual signal like the litter box when constructing explanations (as in Figure 2 (R) bottom). We expect that a lack of robustness to context leads to poor generalizability of both predictions and explanations. If removing or substituting the litter box leads to significantly poorer predictability or explainability, the model or the explanation method is likely unable to predict and detect the cat across a broad range of contexts.

3 Growing readable networks with PiNets

Anatomy of a PiNet We coin **Pointwise-interpretable Networks**⁴ (PiNets) the pseudo-linear networks whose architecture is based on the following components:

1. an **encoder** producing rich encodings $\mathbf{h}(\mathbf{x})$ from input features \mathbf{x} ;
2. a **decoder** producing varying coefficients $\pi(\mathbf{x})$ from rich encodings $\mathbf{h}(\mathbf{x})$;
3. a **second look**, e.g., $\pi(\mathbf{x}) \circ \mathbf{z}$;
4. a linear **aggregator** producing the prediction y .

A diagrammatic representation is provided in Figure 1 (left). When predicting more than one output variable each one has a dedicated set of coefficients. Say we predict p variables denoted by y_k , $k = 1, \dots, p$. Then the decoder must accordingly produce p sets of varying coefficients π_k and the second look is applied to each of them. For each k , and assuming that the aggregator is a summation, we write:

$$y_k = a_k + \sum_* \pi_k(\mathbf{x}) \circ \mathbf{z} \quad (3)$$

³For example, methods like SHAP and LIME require to sample the data locally around $\mathbf{z} \in \mathcal{Z}$ and fit a surrogate model. As this is done locally the estimated coefficients are ultimately functions of \mathbf{z} .

⁴“Pointwise” is used as a synonym of instance-wise.



Design choices A first critical choice in designing PiNets concerns the features. What feature space \mathcal{Z} should explanations be based on? We want features \mathbf{z} to be interpretable. Should \mathcal{X} and \mathcal{Z} coincide? Should \mathcal{Z} be a subspace of \mathcal{X} ? Can their structure be different? Answers to these questions must be tailored to the application.

The design of the encoder-decoder architecture is also crucial, as these components must allow predictive accuracy while, at the same time, shape the structure of explanations. As we show in section 4, the model’s architecture controls its ability to construct meaningful explanations.

The second look may seem mandatory but it can sometimes be relaxed or, equivalently, we can replace the values in \mathbf{z} by ones. We refer to this option as a **soft second look**. The coefficients $\pi(\mathbf{x})$ are still constrained to lie in \mathcal{Z} but no explicit look at features’ values occurs, so that we simply add up the coefficients in the explanation to produce the prediction: $y = \sum_* \pi(\mathbf{x})$. This is a valid approach when the decoder yields the desired structure in $\pi(\mathbf{x})$ and the values \mathbf{z} do not matter in the construction of predictions. For example, when classifying cats and explaining via pixel detection, pixel values may not tell us much about cats in general if their fur color varies across the dataset.

Finally, the aggregator is typically a simple summation as it must ensure pseudo-linearity, and is optionally complemented with shift and scale parameters as needed.

We can further improve the faithfulness of explanations across MARS criteria through enhancements in the training procedure. We now motivate three techniques to this end: recursive stabilization, ensembling, and strong supervision.

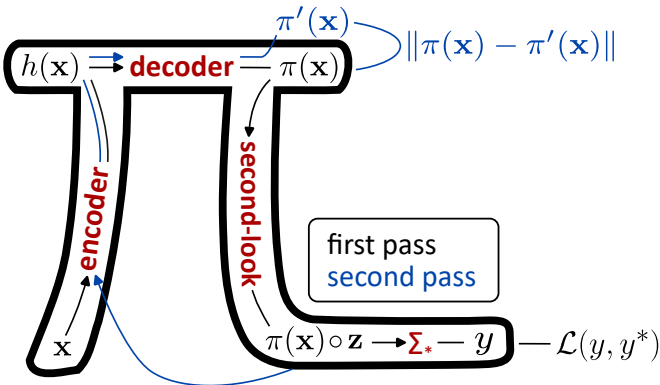


Figure 3: PiNet with recursive feedback. The explanation is used to construct the recursive input $\pi(\mathbf{x}) \circ \mathbf{z}$. The discrepancy between the initial explanation $\pi(\mathbf{x})$ and the recursive explanation $\pi'(\mathbf{x})$ is penalized.

Recursive stabilization As a direct response to the criteria of robustness to context and sufficiency defined in Section 2 we propose a training technique that targets the **recursive stability** of explanations. As illustrated in Figure 3, the loss function is augmented with a feedback on the dissimilarity between the initial explanation $\pi(\mathbf{x})$ and the one generated recursively from $\pi(\mathbf{x}) \circ \mathbf{z}$ as input.⁵

⁵We note that, for this to work, the features \mathbf{z} , and thus the recursive input $\pi(\mathbf{x}) \circ \mathbf{z}$, must be compatible with the encoder, implying that there must be a way to go back from \mathcal{Z} to \mathcal{X} (straightforward when the feature spaces coincide).

Specifically, we penalize the discrepancy between the initial explanation $\pi(\mathbf{x})$ and the recursive explanation $\pi'(\mathbf{x})$ (when $\mathcal{X} \equiv \mathcal{Z}$ we have $\pi'(\mathbf{x}) = \pi(\pi(\mathbf{x}) \circ \mathbf{z})$). In general, our feedback takes the form:

$$\text{Feedback loss } \mathcal{L}_{\text{rec}} = \|\pi(\mathbf{x}) - \pi'(\mathbf{x})\| \quad (4)$$

Minimizing the feedback loss directly pushes explanations to be recursively stable. If $\pi(\mathbf{x})$ abstracts contextual signal from the original input, so that the recursive input $\pi(\mathbf{x}) \circ \mathbf{z}$ is sparse, then recursive stability can directly improve robustness to context. The sparsity of the recursive input indeed translates into the model’s ability to narrow its focus down to the relevant signal in \mathbf{x} when forming explanations $\pi(\mathbf{x})$. If the same relevant signal is available to construct the recursive explanation, we should observe recursive stability in explanations and we expect robustness to context to improve accordingly.

Moreover, since in PiNets predictions are directly built from explanations, recursive stability in explanations implies recursive stability in predictions. Therefore, recursive stability in PiNets’ explanations should let us recover the initial prediction from the recursive input, which translates into sufficiency of explanations.

Ensembling Leveraging multiple models through ensembles is a common strategy to improve predictive accuracy [36, 46–49]. Ensembling can smooth out the errors of each component model, hence improving generalization accuracy. However, it may be at odds with explainability [50–52]. A typical example is random forests, which blend multiple reasonably readable decision trees into an ensemble that becomes painstaking to read.

It follows that an ensemble of neural networks could score low on explainability. But additively ensembling PiNets comes down to linearly combining pseudo-linear models, an operation that preserves pseudo-linearity and thus readability. Furthermore, akin to the improvement of predictive accuracy through averaging, model-specific explanation errors could also be evened out in the ensemble.

Assuming that the aggregator is a summation and that the ensemble is uniformly weighted, we can write an ensemble of M PiNets as follows:

$$\begin{aligned} \bar{y} &= \frac{1}{M} \sum_m y_m = \frac{1}{M} \sum_m \left(a_m + \sum_* \pi_m(\mathbf{x}) \circ \mathbf{z} \right) \\ \Rightarrow \bar{y} &= \left(\sum_m \frac{a_m}{M} \right) + \sum_* \left(\sum_m \frac{\pi_m(\mathbf{x})}{M} \right) \circ \mathbf{z} \\ \Rightarrow \bar{y} &= \bar{a} + \sum_* \bar{\pi}(\mathbf{x}) \circ \mathbf{z} \end{aligned} \quad (5)$$

Notice how the ensemble collapses into a single PiNet with aggregated coefficients $\bar{\pi}(\mathbf{x})$ and shift parameter \bar{a} , effectively preserving readability and alignment.

Strong supervision When available, ground-truth attributions π^* can be used to supervise the training of PiNets. To this end, the training dataset is augmented with ground-truth explanations and an attribution loss



capturing the meaningfulness (accuracy) of model explanations $\pi(\mathbf{x})$ is added to the prediction loss used to supervise training. Depending on the context, this can be a cross-entropy loss, a Dice loss [53, 54], or a distance-based loss. For example, in the latter case we could write, generically:

$$\text{Attribution loss } \mathcal{L}_{\text{att}} = \|\pi(\mathbf{x}) - \pi^*\| \quad (6)$$

We refer to this process as strong supervision. Although beyond the scope of this paper, we would like to highlight that supervising the construction of explanations offers an effective avenue to pursue the designer’s objectives. This represents an important opportunity to improve the quality of explanations according to given desiderata (e.g., their fairness), but it also poses a risk, as conflicting interests may bias the explanations.

4 Evaluating the potential of PiNets

ToyShapes We generate synthetic datasets consisting of images divided into quadrants, within each of which a geometric shape may be drawn (square, triangle, or circle). Heterogeneity is introduced in the shades of gray for both the background and the shapes, as well as in the size of the shapes, and we let one quarter of the shapes be non-filled (outlined). Examples can be found in Figures 1 (right) and 8.

We consider a binary classification task where the positive class corresponds to the presence of at least one triangle in the image. A single logit y is constructed and the predicted class is obtained through a simple thresholding operation $\tilde{y} = \mathbb{1}(y > 0) \equiv \mathbb{1}(\text{Sigmoid}(y) > 0.5)$. We set $\mathcal{Z} \equiv \mathcal{X}$, meaning that we construct explanations in the input space. Explanations, whether aligned or not, take the form of **attribution maps** $\hat{\pi} \in \mathcal{Z}$ and are expected to detect the pixels shaping triangles. Synthetic datasets like ToyShapes come with the ground-truth attributions π^* , allowing us to precisely evaluate the meaningfulness of explanations.

In PiNets, attribution maps $\pi(\mathbf{x})$ are produced by the decoder. In the ToyShapes settings, we let the decoder culminate in a sigmoid transformation such that $\pi_d(\mathbf{x}) \in [0, 1], \forall d$. We grant the model additional flexibility by allowing it to learn both a global intercept a and a global scale parameter b . We constrain $g(\pi, \mathbf{z})$ to be increasing in the coefficients by squaring the scaling parameter. This simplifies interpretation across models: coefficients close to 0 always translate into low pixel importance and vice versa. The resulting **binary PiNet classifier** takes the form:

$$y = a + b^2 \sum_* \pi(\mathbf{x}) \circ \mathbf{z} \quad (7)$$

Note that the functional form above is tailored to the prediction problem at hand and to the structure of the desired explanations. This is one special case of the PiNets modeling framework whose scope extends beyond image classification and pixel detection.

Back to our PiNet classifiers, we can eventually combine M such models into an ensemble, producing the aggregate attribution map:

$$\bar{\pi}(\mathbf{x}) = \frac{1}{M} \sum_m b_m^2 \cdot \pi_m(\mathbf{x}) \quad (8)$$

Experimental settings We compute Grad-CAMs [28] over convolutional neural networks (CNNs [55]) by way of baseline explanations. Grad-CAMs are known to deliver state-of-the-art feature attributions in image classification tasks and pass fundamental sanity checks according to Adebayo et al. [30]. The CNN architecture of the baseline models is the same as in the encoder of the PiNet models we evaluate. Alongside the baseline approach six PiNet variants are considered:

- **Grad-CAM** — CNN + Grad-CAM
- **PiNet Naive** — PiNet with inadequate decoder
- **PiNet Soft** — PiNet with soft second look
- **PiNet** — default PiNet
- **PiNet Feedback** — PiNet with recursive feedback
- **PiNet Ensemble** — ensemble of PiNets
- **PiNet Strong** — strongly-supervised PiNet

The default PiNet • comprises an adequate decoder,⁶ a hard second look, no recursive feedback, and no strong supervision.

To probe results stability, we train 30 CNNs for the baseline and 30 PiNets of each variant, as well as 30 ensembles composed of 10 default PiNets each. Both the training data (1,000 examples) and model parameters are reinitialized at each run with a different random seed. Each time, a 20% validation set is held out from the training data and the model is trained for up to 50 epochs unless validation accuracy reaches 100% earlier. Otherwise, the last model checkpoint is saved only if validation accuracy is greater than or equal to 98%. Strongly-supervised PiNets receive 25 ground-truth attribution maps π^* in addition to the 800 class labels, corresponding to exactly one map per step within each training epoch (the batch size is 32).⁷

Post-processing of attributions By construction, PiNets’ coefficients lie in $[0, 1]$. For Grad-CAMs, we obtain the best results by zeroing out negative gradients (a common practice). Subsequently, and for both approaches, attribution maps are normalized in $[0, 1]$ through a division by the maximum coefficient or gradient observed on the

⁶The decoder is symmetric to the encoder and composed of transposed convolutions, akin to fully convolutional networks [56].

⁷Other hyperparameters governing model architectures and the training procedure can be found in the code repository.



test set,⁸ composed of 1,000 held-out examples (different from the validation sets).

We consider two approaches to post-process attribution maps when producing the final explanations. The **naive post-processing** approach follows the procedure described above and yields continuous attributions $\hat{\pi}_d(\mathbf{x}) \in [0, 1]$. In contrast, the **optimal post-processing** approach binarizes the “naive” attribution maps using a threshold $t \in [0, 1]$ tuned to maximize a detection score reflecting meaningfulness (defined later in eq. (11)). This second approach yields binary attributions $\hat{\pi}_d(\mathbf{x}) \in \{0, 1\}$. Examples of attribution maps can be found in Figures 1 and 8.

Threshold fine-tuning — the optimal post-processing approach — is performed on the test set.⁹ Later, we address the limiting nature of the assumption underlying the feasibility of thresholding; namely, that ground-truth maps π^* are readily available such that we can quantify meaningfulness.

Meaningfulness Explanations are attribution maps $\hat{\pi} : \mathcal{X} \rightarrow \mathcal{Z}$ and we gauge their meaningfulness through their attribution accuracy with respect to binary ground-

truth attributions π^* . Analogous to performance indicators used in binary classification, we distinguish between two types of errors. The **True Detection Rate** (TDR) parallels the true positive rate (*aka* sensitivity or recall); its complement represents the miss rate. A low TDR indicates that the method fails to detect the relevant signal. The **True Abstraction Rate** (TAR) parallels the true negative rate (*aka* specificity); its complement represents the false alarm rate. A low TAR indicates that the method fails to filter out irrelevant and spurious signal.

To accommodate both naive (continuous) and optimal (binary) post-processing approaches, we define and combine the TDR and TAR for any instance $\mathbf{x} \in \mathcal{X}$ and their associated maps $\pi(\mathbf{x}) \in [0, 1]^D$ and $\pi^* \in \{0, 1\}^D$ ($D = \dim(\mathcal{Z})$) as follows:

$$\text{TDR} = \frac{\sum_* \pi^* \circ \hat{\pi}(\mathbf{x})}{\sum_* \pi^*} \quad (9)$$

$$\text{TAR} = \frac{\sum_* \neg \pi^* \circ \neg \hat{\pi}(\mathbf{x})}{\sum_* \neg \pi^*} \quad (10)$$

$$\text{Detection-Score} = \overline{\text{TDR}} \times \overline{\text{TAR}} \quad (11)$$

Where π^* is the ground-truth binary attribution map

⁸Dataset-wide normalization was found to perform better than instance-wise or batch-wise normalization.

⁹Note, moreover, that models are selected based on their predictive accuracy only and no measurement of meaningfulness is performed during training.

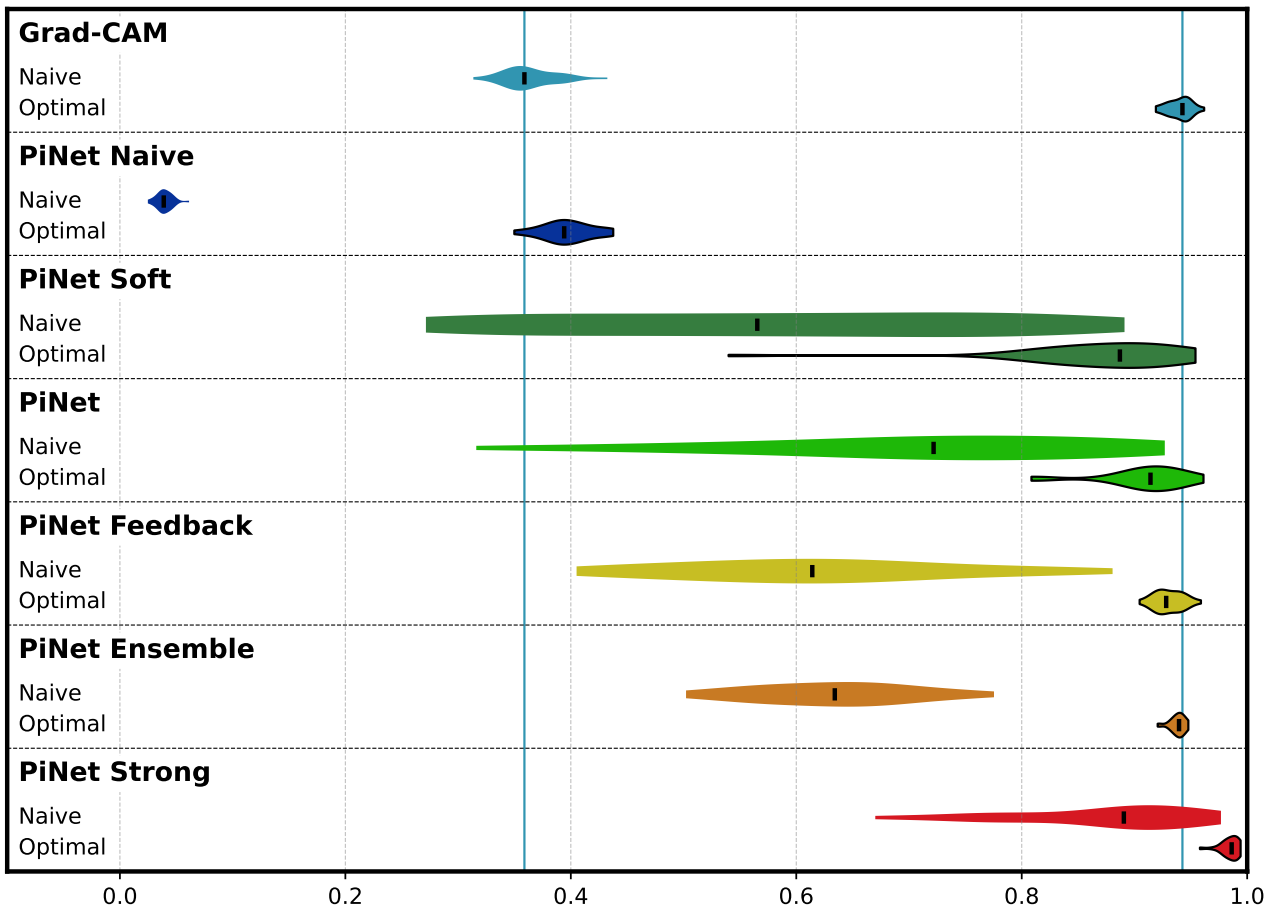


Figure 4: Distribution of meaningfulness in ToyShapes depicted by violin plots. Marks inside each violin represent medians. Blue vertical lines extend the medians of the baseline (Grad-CAMs). “Naive” and “Optimal” refer to the post-processing approach.



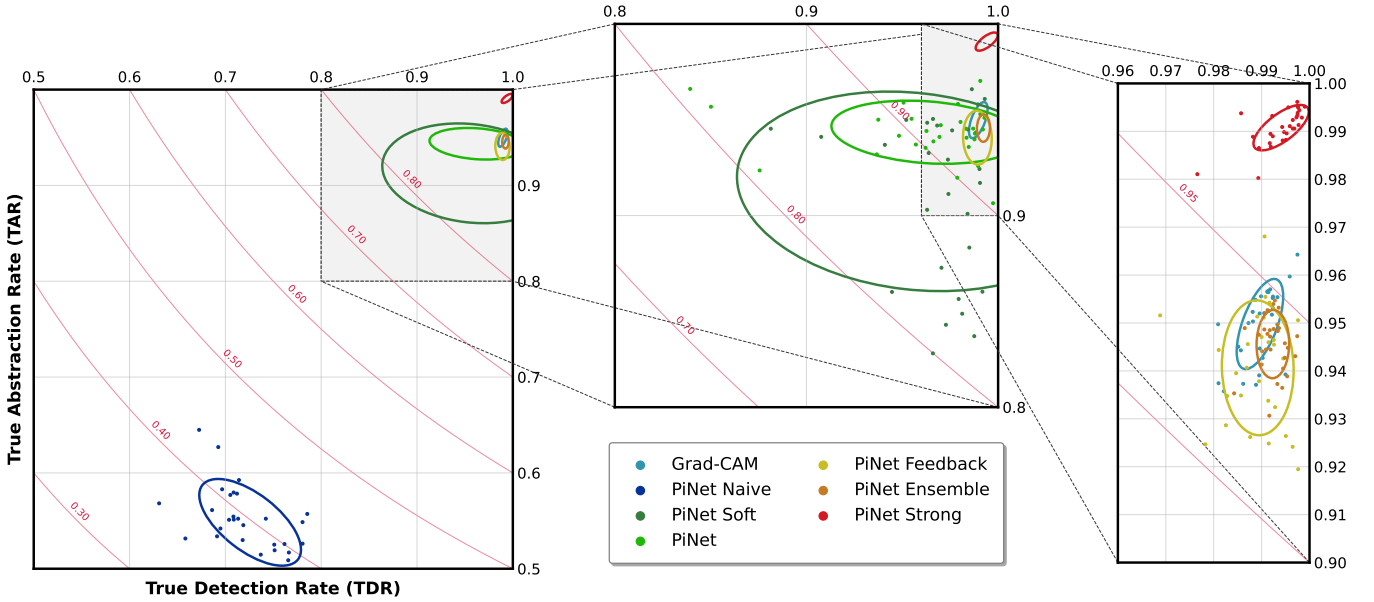


Figure 5: Meaningfulness under the optimal post-processing approach (thresholding) in ToyShapes. Red contours show iso-levels of the detection score (eq. (11)). Points represent fitted models color-coded by group, and are shown together with 95% Gaussian confidence ellipses. Ellipses inside the gray insets (left and middle panels) are shown without points for visual clarity; middle and right panels magnify such insets showing the points.

and the operator \neg denotes the complement ($1 - \cdot$) of the object it precedes; that is, $\neg\pi$ is the negative image of π . Instance-wise TDRs and TARs are averaged over the test set ($\overline{\text{TDR}}, \overline{\text{TAR}}$), and the detection score is the product of these averages. This composite indicator rewards balance between sensitivity and specificity, and carries a useful interpretation: for any value $\alpha \in [0, 1]$ taken by the detection score, both components (TDR and TAR) are guaranteed to be greater than or equal to α , since they are both in $[0, 1]$.

Results from ToyShapes experiments are summarized in Figure 4, and a detailed view of performance under the optimal post-processing approach is provided in Figure 5.

PiNets equipped with an inadequate decoder (● PiNet Naive) show very poor detection performance,¹⁰ even though they achieve high predictive accuracy — as can be observed in Figure 7. Even if aligned, explanations that do not convey meaningful cues in the data are not interpretable and thus of little value. This sheds light on the fact that meaningful explanations are not a precondition to predictability by default. Predictive accuracy indicates that the model has acquired some degree of statistical intelligence but it is our mission to make the model capable of conveying it in a way that is meaningful to us.

A careful design of the encoder-decoder architecture serves this purpose: forcing the model to produce meaningful explanations and make accurate predictions out of them. The model architecture, in addition to enabling learning, also acts as a constraint on the structure of the explanations $\pi(x)$. The much higher meaningfulness of explanations produced by the soft second look variant (● PiNet Soft), equipped with an adequate decoder, supports this idea. Without an explicit second look the model’s ability to detect shapes depends on the structure induced

by the decoder. If the decoder did not constrain the model to construct meaningful explanations, the model would most likely produce random-looking attribution maps as in the case of the ● PiNet Naive variant.

The quality of explanations and the stability of results across the thirty fitted models are improved by the implementation of an explicit second look (default ● PiNet) as exemplified by the breadth of the violin plots in Figure 4. This is especially striking with the optimal post-processing approach as can be seen in the size of the ellipses in Figure 5.

Still in the optimal scenario, recursive feedback (● PiNet Feedback) and ensembling (● PiNet Ensemble) both contribute to improving the meaningfulness of explanations and the stability across fitted models — bringing PiNets’ performance to a level comparable to that of ● Grad-CAMs. Strong supervision (● PiNet Strong) yields the most striking improvements, with explanations after thresholding close to perfect.

Fine-tuning effort In the scenario of optimal post-processing (thresholded attribution maps) PiNets therefore require additional training techniques to perform on par with the baseline. This, however, does not hold true in the naive post-processing scenario, wherein even the ● PiNet Soft variant tends to perform better than ● Grad-CAMs. As a matter of fact, the feasibility of optimal post-processing relies on the availability of ground-truth attribution maps π^* — an assumption rarely met in real-world applications. When meaningfulness is hard to quantify, thresholding may still be applied but limited to qualitative (e.g., visual) inspection of the explanations. We attempt to assess how difficult such an approach is in practice.

¹⁰A closer look at the attribution maps would in fact reveal random-looking attributions.



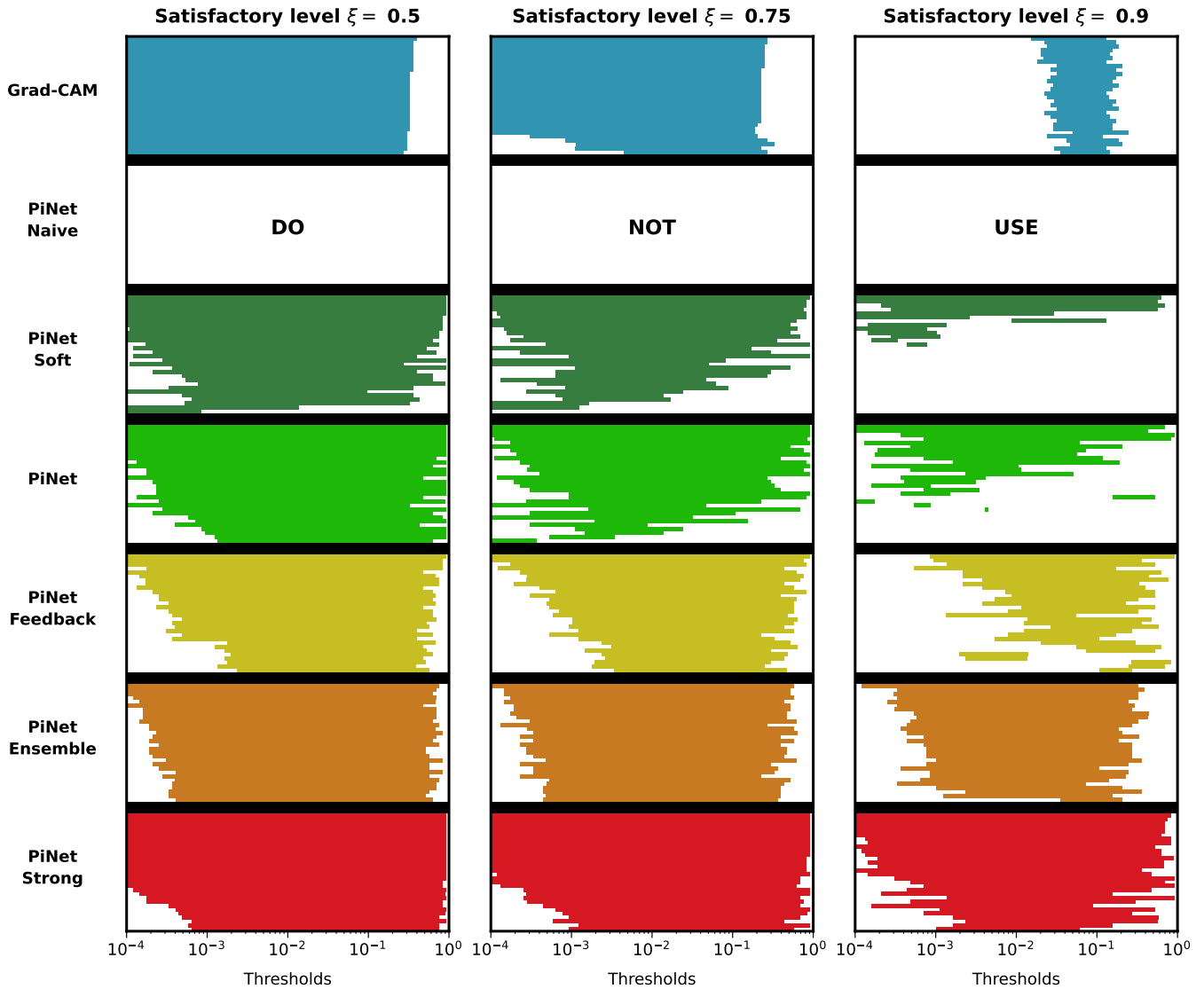


Figure 6: Ease of fine-tuning meaningfulness in ToyShapes. Bars represent the ranges of thresholds satisfying a detection score of at least ξ (in the column title). Thresholds reported on the x-axis are log-transformed and range from 10^{-4} to 1. Within each model group, results are sorted by the breadth of the range, for clarity. The \bullet PiNet Naive variant is flagged “do not use” as it yields spurious explanations for any threshold $t \in [0, 1]$.

To do this, we set an arbitrary *satisfactory level* ξ for the detection score and count the thresholds $t \in [0, 1]$ for which the detection score is greater than or equal to ξ . We can then gauge the ease with which one can fine-tune the threshold by visualizing on a log scale¹¹ the range of thresholds that yield satisfactory attributions. The wider the range, the easier it should be to converge on satisfactory detection quality.

The ranges of thresholds for which the detection score is satisfactory with respect to $\xi \in \{0.5, 0.75, 0.9\}$ are reported in Figure 6. \bullet Grad-CAMs provide a very strong baseline for levels 0.5 and 0.75, and \bullet default PiNets perform slightly worse, notably in terms of stability across the 30 fitted models. However, \bullet recursive feedback, \bullet ensembling and \bullet strong supervision offer substantial improvements, making PiNets less dependent on the choice of threshold. Moreover, Grad-CAMs appear to fall behind

at the 0.9 level — with a comparatively small range of thresholds leading to satisfactory detection quality. While not all fitted PiNets beat Grad-CAMs in terms of detection quality, those that do are easier to fine-tune, especially at the $\xi = 0.9$ level. And this observation becomes more stable across fitted models as we improve upon the default configuration.

We conclude that PiNets do not require substantial fine-tuning effort to achieve satisfactory levels of meaningfulness. And we stress again that detection quality tends to be much better prior to fine-tuning in PiNets than in the baseline.

Sufficiency and Robustness A thorough evaluation of robustness to context is beyond the scope of this paper and would require a dedicated and extensive experimental protocol. However, we can capture some of it as well

¹¹In doing so, we seek to mimic the way one would typically fine-tune the threshold manually.



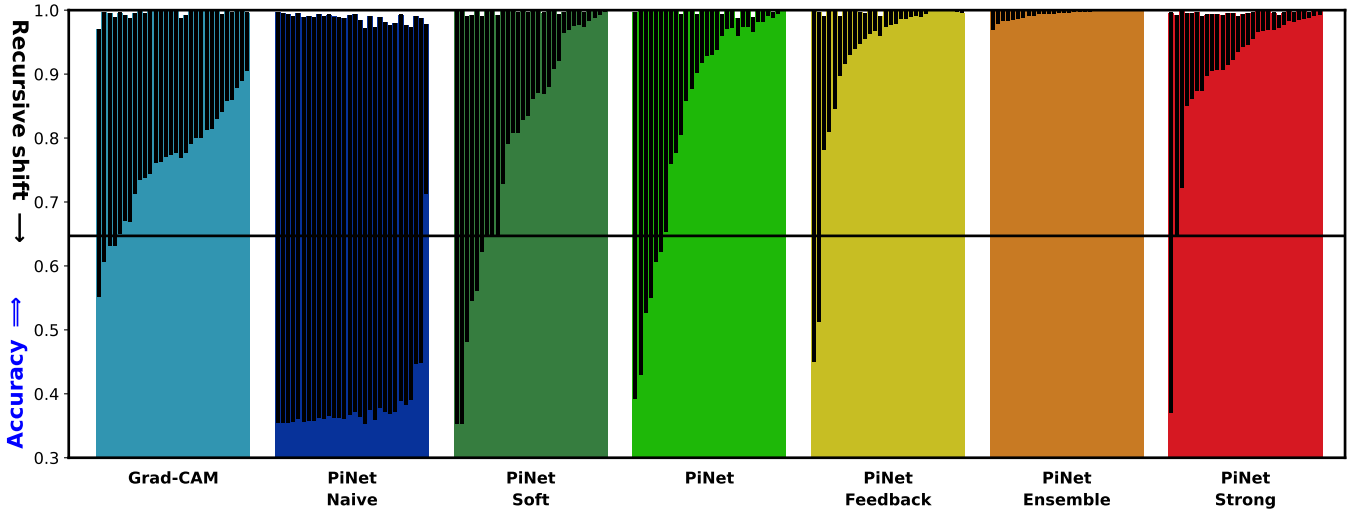


Figure 7: Recursive accuracy shift in ToyShapes. The bars in each panel represent the model’s test predictive accuracy (note that the vertical axis starts at 0.3). The black sticks represent recursive accuracy shifts; they start at the model’s accuracy level on top, and extend downwards to reach the accuracy levels achieved after recursion. The horizontal black line shows the naive predictive accuracy level achieved by always predicting the dominant class (presence of triangles). Recursive accuracy below this level indicates a tendency to predict the absence of triangles from the recursive input, a sign of gross insufficiency of explanations.

as sufficiency through an analysis of the recursive stability of predictions.

We compute the accuracy shift under recursive prediction; that is, the change in predictive accuracy when predicting from the filtered signal $\hat{\pi}(\mathbf{x}) \circ \mathbf{z}$ compared to the original signal \mathbf{x} ($\equiv \mathbf{z}$ here). To be sufficient, an explanation must detect signals so as to recover the prediction if predicting from it. A lack of sufficiency would be reflected in distorted recursive predictions and thus in a change in predictive accuracy (most likely a drop).

Besides, a lack of robustness to context can be responsible for discrepancy between the initial and the recursive explanations. Because in PiNets this implies recursive instability of predictions, robustness can also be captured by recursive accuracy shifts.

Results are reported in Figure 7. While the accuracy of initial predictions is very high for all candidates, recursive accuracy shifts behave rather differently across groups. As a preliminary note, we expect a tendency to observe drops in predictive accuracy under recursion since a recursive input $\pi \circ \mathbf{z}$ is usually a distorted and sparser version of the original input \mathbf{x} . Sufficient explanations should mitigate the accuracy drop.

As for the results, while PiNets equipped with an inadequate decoder (● PiNet Naive) are accurate in their predictions, their explanations are clearly insufficient, as evidenced by the large accuracy shifts. Substantial heterogeneity appears across almost all other variants. ● Ensembling is the positive outlier; in addition to having the smallest shifts, it has by far the least variable. Through averaging, the ensemble’s attributions highlight what is agreed upon across the different models, which is more likely to contain sufficient relevant signal. Next best, both in terms of shift size and variability, is the ● recursive feedback variant.

Besides these preliminary insights a more sophisti-

cated experimental set-up — closer to the notion of robustness to context — will be necessary to understand the effect of recursive stabilization on the quality of explanations and their robustness across different contexts or following distribution shifts.

Structural explainability In the ToyShapes experiment, PiNets equipped with a naive decoder achieve high predictive accuracy but produce spurious explanations — demonstrating how a model may in fact find its way to good predictions through explanations that are uninformative for the user. Jethani et al. [18] indeed found that a prediction can sometimes be encoded in its associated explanation, a finding obtained while experimenting with models showing a non-negligible computational distance between predictions and explanations [14, 17]; i.e., the function $g(\pi, \mathbf{z})$ is complex. It is then no wonder that an unconstrained PiNet encodes predictions in explanations, hence in the last layer: the prediction is simply passed from the encoder to the aggregator and through the decoder without it organizing the acquired intelligence into explanations.

In contrast, when equipped with an adequate decoder, PiNets learn to detect triangles without supervision on the explanations. In these settings, meaningful explanations become a precondition to predictive accuracy. Once more, the decoder plays a key role in PiNets. It acts as a constraint on the space of possible explanations, thereby guiding the model towards meaningful explanations when carefully designed. While the encoder drives the acquisition of statistical intelligence, encoded in $\mathbf{h}(\mathbf{x})$, the decoder imposes an interpretable structure on $\pi(\mathbf{x})$, pushing the model to organize the acquired intelligence into explanations that capture meaningful cues in the data.

This property raises an important question: to what



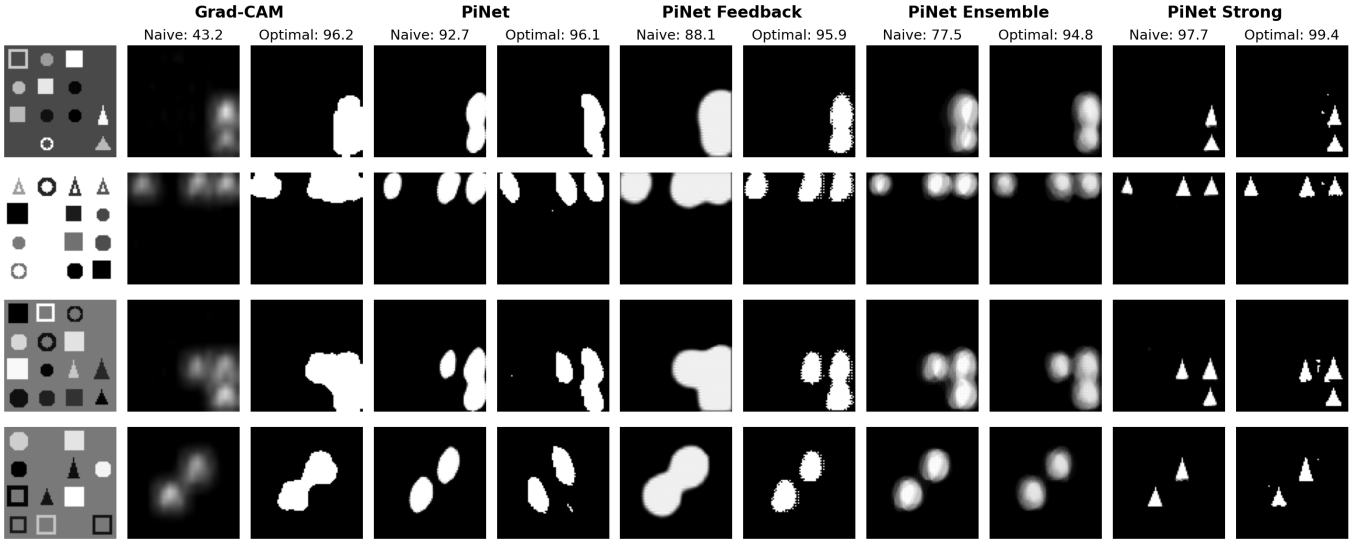


Figure 8: Test attribution examples in ToyShapes for the top explainer (w.r.t. meaningfulness) of each model group.

degree of meaningfulness can PiNets organize their explanations? The limited sharpness of the attribution maps we obtain in the ToyShapes experiment is in part due to the prediction task; a simple classification problem wherein only the presence of triangles matters. In this type of settings, maximizing predictive accuracy requires only producing a logit. There can thus be many decision boundaries that achieve the same accuracy level and such equi-accurate PiNets would be characterized by different degrees of explanatory faithfulness. Converging to highly meaningful explanations is therefore far from guaranteed.

What would happen if we fitted PiNets to more informative target variables that further constrain the model in the way predictions are constructed? Would PiNets be constrained to form better explanations despite the absence of supervision on the explanations?

Flood mapping To investigate this question, we turn to a semantic segmentation problem on a real-world dataset where the objective is to detect flooded areas from satellite images. Due to its complexity, the task is not well addressed by learning to predict and explain class labels, as in the case of ToyShapes. The detection of flooded areas typically requires the availability of high-quality hand-annotated segmentation maps as proxy for ground-truth maps π^* .

We use the Sen1Floods11 dataset [57], which was curated for flood mapping from Sentinel scenes. Images in this dataset are hand-annotated with three pixel classes: water (1), not water (0), and no data or not valid (-1). The latter class comprises absence of data in the satellite images and other conflicts like the presence of clouds. Segmentation models, usually taking the form of encoder-decoder architectures, can be trained to classify each pixel [56, 58]. We follow this approach to train a baseline model that we call SegNet.

In addition, we train a PiNet to predict the surface area of flooded and non-flooded regions. For this purpose, response variables $\mathbf{y} = \{y_{-1}, y_0, y_1\}$ are constructed

to represent the number of pixels occupied by each class in the image. The regression is therefore performed based on image-level information, whereas the SegNet is exposed to ground-truth attribution maps that embed pixel-level information. In this respect and in line with the terminology used in the discussion of the ToyShapes experiments, the SegNet can be seen as a PiNet that is exclusively strongly supervised (on π^*), whereas the PiNet is not and instead is trained to predict \mathbf{y} .

The same encoder-decoder architecture is shared by both the SegNet and the PiNet, as well as training settings. The backbone encoder is a lightweight version of the geospatial foundation model Prithvi [59, 60], while the decoder is a UperNet [61]. Only the decoder is trained as we freeze the pretrained weights of the encoder. The PiNet is only equipped with a soft second look and is, in fact, a SegNet augmented with an aggregator enabling regression on \mathbf{y} .

We let \mathcal{Z} be a matrix space whose dimensions correspond to the height and width of the satellite images, while the input space \mathcal{X} has six bands of same dimensions. For any pixel d , a soft classification is produced from a softmax normalization of the decoder’s output, yielding $\pi_d \in [0, 1]^3$ such that $\sum_k \pi_{d,k} = 1$ and $\sum_d \sum_k \pi_{d,k} = |\mathcal{Z}|$, i.e., the number of pixels in the image. Then, PiNets’ predictions on \mathbf{y} simply take the form $y_k = \sum_* \pi_k(\mathbf{x}), \forall k$. In the final segmentation maps used for visualization, each pixel is assigned the class with highest probability.

For the water and no-water classes we report the true detection rate (TDR) defined in eq. (9) and the intersection-over-union (IoU), which is defined for each class k as:

$$\text{IoU}_k = \frac{\sum_* \pi_k(\mathbf{x}) \circ \pi_k^*}{(\sum_* \pi_k(\mathbf{x}) + \pi_k^*) - (\sum_* \pi_k(\mathbf{x}) \circ \pi_k^*)} \quad (12)$$

In addition, the mean absolute error (MAE), used as the loss function to train the PiNet, is reported for the



water class.¹² Results computed on a held-out test set are summarized in Table 1.

The detection of non-flooded areas is comparable between the two models. For flooded areas, however, the SegNet outperforms the PiNet, especially in terms of IoU, which is expected given the greater granularity of pixel-level class labels over image-level surface areas. Yet, as can be appreciated in the examples in Figure 9, the difference is not dramatic and the PiNet is able to produce meaningful segmentation maps. Note that these results are obtained for the simpler variant of PiNets and therefore likely reflect a lower bound on the potential of PiNets in this context.

Two important insights come out of this. First, they confirm that well-designed PiNets constrain explanations to be meaningful in order to produce accurate predictions — as exemplified by the greater sharpness of attribution maps in the context of regression. Second, the potential

of PiNets in semantic segmentation suggests that they could be useful in real-world problems where target variables descriptive of the input data are more affordable and readily available than full annotations of the latter.

	Water			No water	
	MAE ↓	IoU ↑	TDR ↑	IoU ↑	TDR ↑
SegNet	2582	0.332	0.904	0.814	0.940
PiNet	1110	0.256	0.802	0.819	0.959
Delta	-57.0%	-22.9%	-11.3%	+0.6%	+2.0%

Table 1: Performance in flood mapping. The level of improvement (green) or deterioration (red) of the PiNet over the SegNet is reported in the Delta row. ↑ and ↓ indicate the higher the better and the lower the better, respectively.

¹²The regression performance is not of great importance here. Yet, if we were to construct estimates of flooded surface areas then the MAE of the water class would be a key indicator; whereas the MAE for the no-water class would be of little relevance. We therefore report only the former.

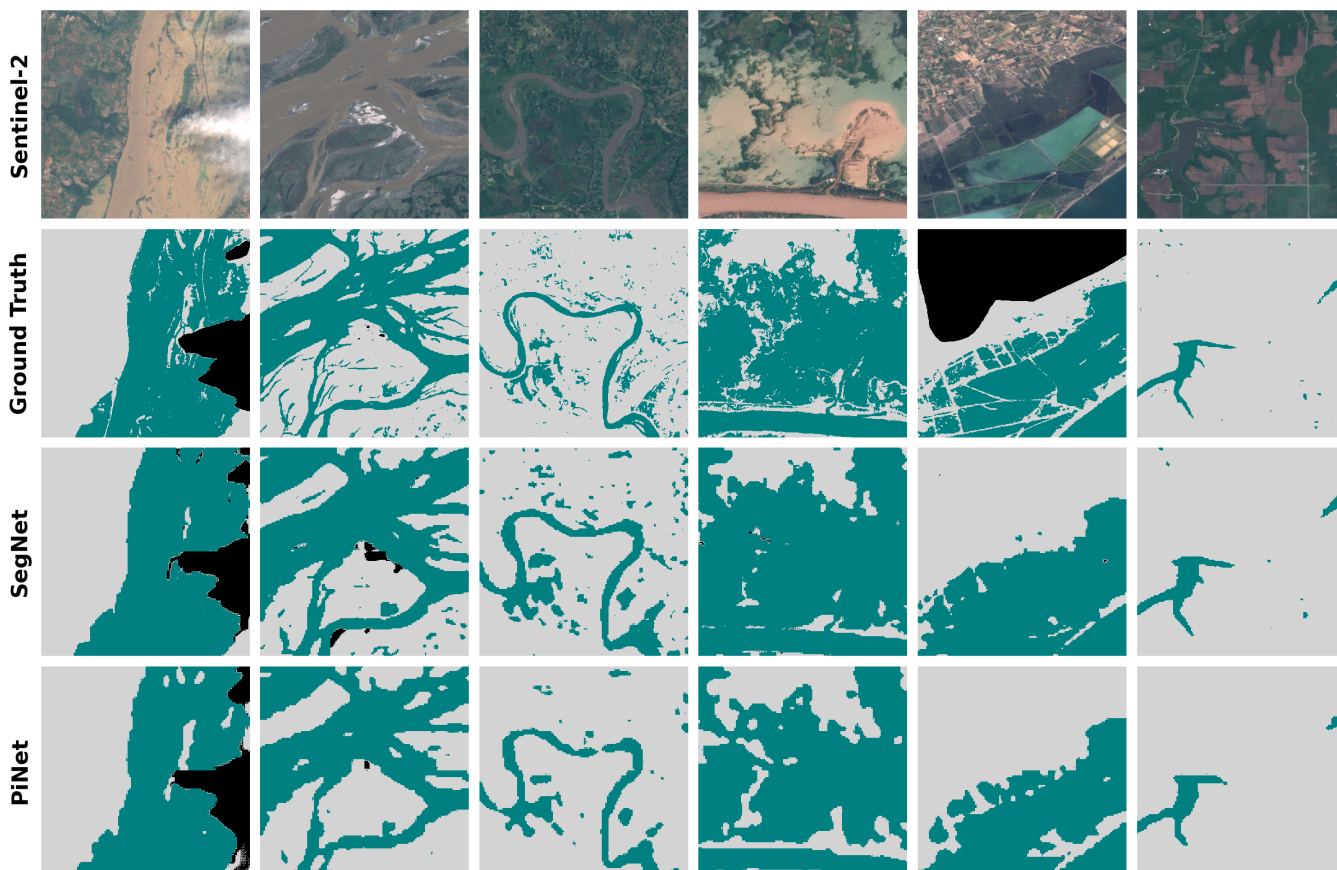


Figure 9: Test segmentation maps in Sen1Floods11. From top to bottom: Sentinel-2 images (RGB bands), hand-annotated maps (proxy for ground-truth), SegNet segmentation maps, and PiNet attribution maps. Classes $k = \{-1, 0, 1\}$ are assigned, respectively, the colors black (no data/not valid), gray (no water) and teal (water).



5 Discussion

Summary In this paper we started by identifying forms of misalignment in several important explainability methods. Misalignment can hinder the trustworthiness of explanations, as they may not mirror the model’s prediction-making process or do so ambiguously. We argued that explanatory alignment requires, on the one hand, that explanations be intrinsic to the model and, more strictly, that they immediately precede predictions in the model architecture and, on the other hand, that the features leveraged in explanations be fully interpretable. We then articulated the principle of model readability as a means to enforce explanatory alignment by design and argued that pseudo-linear neural networks can serve as a basis to achieve readability in deep learning settings. Such models produce linear predictions instance-wise such that, even though the model is not linear, its predictions are linearly readable.

We presented and evaluated PiNets, a modeling framework for the design of pseudo-linear networks. While PiNets are easily made readable (and thus aligned) thanks to their pseudo-linear structure, they must be carefully designed and trained in order to score high on the other faithfulness criteria. We propose and consider the MARS evaluation framework, composed of four criteria: meaningfulness, alignment, robustness to context and sufficiency.

Using a synthetic image dataset and a binary classification task to evaluate PiNets on these criteria we found that modeling choices play a key role in the performance of PiNets. Notably, the model architecture must be carefully designed to let PiNets both acquire sufficient statistical intelligence (encoder) and communicate it in an interpretable structure (decoder).

We also found that a variety of training techniques can be tailored to further improve faithfulness. In particular, we showed that the implementation of a recursive feedback loss stabilizes explanations and improves their sufficiency, robustness to context, as well as their meaningfulness. Moreover, we exploited the chimeric explainer-predictor nature of PiNets to augment training with a limited amount of ground-truth attribution maps. This strong supervision strategy strikingly enhanced faithfulness. Finally, we showed that ensembling multiple PiNets produces marked improvements in faithfulness while preserving the pseudo-linearity and readability of the ensemble model.

In terms of meaningfulness of the explanations, PiNets were competitive against Grad-CAMs computed on CNN models when using the optimal post-processing approach (fine-tuned thresholding). Since this approach may be limited to qualitative (e.g., visual) inspection in practice, we also considered a naive (non-thresholded) post-processing approach. With it, even less sophisticated PiNet variants outperformed Grad-CAMs. We assessed the ease of fine-tuning the threshold and found that, when targeting high-quality explanations, PiNets are less de-

pendent on threshold selection and may thus be easier to fine-tune qualitatively or under limited resource constraints.

To evaluate the sufficiency and robustness of explanations, we evaluated accuracy shifts under recursive prediction. Again, PiNets performed well compared to Grad-CAMs, with ensembling standing out as a particularly effective technique. Ensembling indeed has a stabilizing effect on both predictions and explanations.

Finally, we assessed the ability of PiNets to organize their explanations when learning to predict variables that are more informative than class labels. To this end, we trained a PiNet to predict the surface areas of flooded and non-flooded regions and to explain these predictions with attribution maps (taking the form of segmentation maps). Encouragingly, the PiNet performed reasonably well compared to a baseline model designed to perform segmentation and trained directly with pixel-level information.

Outlook Because of their ability to simultaneously form predictions and explanations, PiNets can be effective across a variety of tasks. For example, segmentation problems where annotated segmentation maps are scarce are usually tackled by using weak labels such as class labels [62, 63] in addition to annotated maps. Training a PiNet would bypass the complexities of the multi-step training procedures required for this type of hybrid supervision. Also, as illustrated in the flood-mapping exercise, PiNets could be useful in contexts where target variables descriptive of the input data are more affordable and readily available than pixel-level annotations.

Besides, in the context of prediction problems, strong labels can be used to sharpen explanations through strong supervision. It must however be emphasized that influencing explanations through strong supervision is a double-edged sword: it may raise ethical concerns if the construction or sampling of ground-truth attributions is biased while it also offers the opportunity to mitigate such biases. This is equivalently pertinent in tabular data settings where demographic variables can populate the feature space and be leveraged in explanations, potentially producing explanations that reflect or reinforce demographic biases. One could explore the use of strong supervision to mitigate such biases and produce explanations that achieve greater standard of fairness.

Extending PiNets to other data structures such as audio, text, graphs or genomic sequences is another promising avenue for future developments. Because we can tap into the great flexibility afforded by neural networks, we believe PiNets can be adapted to a wide variety of data types and prediction tasks. Furthermore, significant additional flexibility is offered by the use of two feature spaces, \mathcal{X} and \mathcal{Z} . While the input features (\mathcal{X}) shall typically play the same role as in standard neural networks (i.e., fuel statistical intelligence), the features leveraged in explanations (\mathcal{Z}) can be tailored to suit a variety of de-



sign, research, or application needs. For example, in the context of audio data, one could use raw waveforms as input data but form explanations in a spectrogram space. In the context of graph data, one could leverage more potent graph neural networks, so as to capture topological intricacies, but read simpler structures out of them, e.g., forming explanations in terms of node degrees or centrality measures. In genomic applications, one could train the model on raw sequence data while forming explanations in terms of known motifs or abundances of functional elements.

It is noteworthy that different data structures require different definitions of explanatory meaningfulness. When feature attribution comes down to a detection exercise, we can straightforwardly imagine what ground-truth attribution maps should capture. In many other settings, however, the definition of meaningfulness is less straightforward and may require a more careful conceptualization. For example, oftentimes in the context of tabular data meaningful explanations may need to capture causal relationships, which are often the object of debate in real-world applications. Intrinsic explanations would still be aligned with the model’s reasoning but risk capturing spurious relationships.

Lastly, it would be worth investigating the robustness to context of explanations more thoroughly, along with the effect of stabilizing the explanations recursively.

While it has become common to study the sensitivity of predictive performance to distribution or domain shifts [64, 65] and adversaries [66], the robustness of explanations has received less attention and is still poorly understood. One could investigate the feasibility and effectiveness of incorporating existing robustness-enhancing techniques, such as adversarial training [67], into PiNets — with the aim of robustifying not only the predictions, but also the explanations. Relatedly, strong supervision on ground-truth attributions could be explored in conjunction with mixture-based data augmentation techniques [68, 69] applied directly to strong labels. This should improve the model’s robustness to context and thus performance under distribution shifts.

Notes Complete code for the generation of the synthetic data and the reproduction of the results is available in the Github repository: <https://github.com/FractalSyn/PiNets-Alignment>. We used PyTorch for the implementation and training of the deep learning models [70] and the Adam algorithm [71, 72] for optimization.

Acknowledgments We are thankful to S. Bianchini (Unistra), B. Gulhan (Penn State), M. Laguerre (EM Lyon), R. Porcedda (Sant’Anna), and L. Testa (Carnegie Mellon) for their insightful comments and suggestions on the manuscript.

References

- (xAI): Concepts, taxonomies, opportunities and challenges toward responsible AI. *Information Fusion*, 2020.
- [1] L. Festinger. *A theory of cognitive dissonance*. Stanford University Press, 1957.
- [2] R. E. Nisbett and T. D. Wilson. Telling more than we can know: Verbal reports on mental processes. *Psychological Review*, 1977.
- [3] P. Johansson, L. Hall, S. Sikstrom, and A. Olsson. Failure to detect mismatches between intention and outcome in a simple decision task. *Science*, 2005.
- [4] Z. C. Lipton. The mythos of model interpretability: In machine learning, the concept of interpretability is both important and slippery. *Communications of the ACM*, 2018.
- [5] C. Rudin. Stop explaining black box machine learning models for high stakes decisions and use interpretable models instead. *Nature Machine Intelligence*, 2019.
- [6] R. Guidotti, A. Monreale, S. Ruggieri, F. Turini, F. Giannotti, and D. Pedreschi. A survey of methods for explaining black box models. *ACM Computing Surveys*, 2018.
- [7] A. Barredo Arrieta, N. Díaz-Rodríguez, J. Del Ser, A. Bennetot, S. Tabik, et al. Explainable artificial intelligence
- [8] R. Marcinkevičs and J. E. Vogt. Interpretable and explainable machine learning: A methods-centric overview with concrete examples. *WIREs Data Mining and Knowledge Discovery*, 2023.
- [9] C. Molnar. Interpretable machine learning, 2025.
- [10] S. M. Lundberg and S.-I. Lee. A unified approach to interpreting model predictions. *NeurIPS*, 2017.
- [11] M. T. Ribeiro, S. Singh, and C. Guestrin. "Why should I trust you?" explaining the predictions of any classifier. In *KDD*. ACM, 2016.
- [12] V. Petsiuk, A. Das, and K. Saenko. RISE: Randomized input sampling for explanation of black-box models. *BMCV*, 2018.
- [13] M. T. Ribeiro, S. Singh, and C. Guestrin. Anchors: High-precision model-agnostic explanations. In *AAAI*, 2018.
- [14] J. Chen, L. Song, M. Wainwright, and M. Jordan. Learning to explain: An information-theoretic perspective on model interpretation. In *ICML*. PMLR, 2018.
- [15] M. Ivanovs, R. Kadikis, and K. Ozols. Perturbation-based methods for explaining deep neural networks: A survey. *Pattern Recognition Letters*, 2021.
- [16] F. Paissan, M. Ravanelli, and C. Subakan. Listenable maps for audio classifiers. In *ICML*. PMLR, 2024.
- [17] J. Yoon, J. Jordon, and M. Van der Schaar. INVASE: Instance-wise variable selection using neural networks. In *ICLR*, 2018.
- [18] N. Jethani, M. Sudarshan, Y. Aphinyanaphongs, and R. Ranganath. Have we learned to explain?: How interpretability methods can learn to encode predictions in their interpretations. In *ICAIS*. PMLR, 2021.
- [19] X. Zhang, D. Lee, and S. Wang. Comprehensive attribution: Inherently explainable vision model with feature detector. In *ECCV*. Springer, 2024.
- [20] M. Böhle, M. Fritz, and B. Schiele. B-cos networks: Alignment is all we need for interpretability. In *CVPR*. IEEE, 2022.
- [21] M. Vandenhirz and J. E. Vogt. From pixels to perception: Interpretable predictions via instance-wise grouped feature selection. In *ICML*. PMLR, 2025.
- [22] B. Kim, M. Wattenberg, J. Gilmer, C. Cai, J. Wexler, et al. Interpretability beyond feature attribution: Quantitative testing with concept activation vectors (TCAV). In *ICML*. PMLR, 2018.
- [23] P. W. Koh, T. Nguyen, Y. S. Tang, S. Mussmann, E. Pierson, et al. Concept bottleneck models. In *ICML*. PMLR, 2020.



- [24] M. Espinosa Zarlenga, P. Barbiero, G. Ciravegna, G. Marra, F. Giannini, et al. Concept embedding models: Beyond the accuracy-explainability trade-off. *NeurIPS*, 2022.
- [25] V. V. Ramaswamy, S. S. Kim, R. Fong, and O. Russakovsky. Overlooked factors in concept-based explanations: Dataset choice, concept learnability, and human capability. In *CVPR*. IEEE, 2023.
- [26] S. Sinha and A. Zhang. A comprehensive survey on the risks and limitations of concept-based models. *arXiv*, 2025.
- [27] K. Simonyan, A. Vedaldi, and A. Zisserman. Deep inside convolutional networks: Visualising image classification models and saliency maps. In *ICLR*, 2014.
- [28] R. R. Selvaraju, M. Cogswell, A. Das, R. Vedantam, D. Parikh, and D. Batra. Grad-CAM: Visual explanations from deep networks via gradient-based localization. In *ICCV*. IEEE, 2017.
- [29] M. Sundararajan, A. Taly, and Q. Yan. Axiomatic attribution for deep networks. In *International conference on machine learning*, pages 3319–3328. PMLR, 2017.
- [30] J. Adebayo, J. Gilmer, M. Mueley, I. Goodfellow, M. Hardt, and B. Kim. Sanity checks for saliency maps. *NeurIPS*, 2018.
- [31] W. Nie, Y. Zhang, and A. Patel. A theoretical explanation for perplexing behaviors of backpropagation-based visualizations. In *ICML*. PMLR, 2018.
- [32] S. Hooker, D. Erhan, P.-J. Kindermans, and B. Kim. A benchmark for interpretability methods in deep neural networks. *NeurIPS*, 2019.
- [33] Y. Jia, E. Frank, B. Pfahringer, A. Bifet, and N. Lim. Studying and exploiting the relationship between model accuracy and explanation quality. In *ECML PKDD*. Springer, 2021.
- [34] J. Chen, L. Q. R. Ooi, T. W. K. Tan, S. Zhang, J. Li, et al. Relationship between prediction accuracy and feature importance reliability: An empirical and theoretical study. *NeuroImage*, 2023.
- [35] L. Breiman, J. Friedman, R. A. Olshen, and C. J. Stone. *Classification and regression trees*. Chapman and Hall/CRC, 1984.
- [36] L. Breiman. Random forests. *Machine learning*, 2001.
- [37] J. H. Friedman and B. E. Popescu. Predictive learning via rule ensembles. *The Annals of Applied Statistics*, 2008.
- [38] T. Hastie and R. Tibshirani. Varying-coefficient models. *Journal of the Royal Statistical Society Series B: Statistical Methodology*, 1993.
- [39] J. Fan and W. Zhang. Statistical methods with varying coefficient models. *Statistics and its Interface*, 2008.
- [40] D. Alvarez Melis and T. Jaakkola. Towards robust interpretability with self-explaining neural networks. *NeurIPS*, 2018.
- [41] A. Ignatiev, N. Narodytska, and J. Marques-Silva. Abduction-based explanations for machine learning models. In *AAAI*, 2019.
- [42] S. Dasgupta, N. Frost, and M. Moshkovitz. Framework for evaluating faithfulness of local explanations. In *ICML*. PMLR, 2022.
- [43] B. Recht, R. Roelofs, L. Schmidt, and V. Shankar. Do imagenet classifiers generalize to imagenet? In *ICML*. PMLR, 2019.
- [44] A. Ilyas, S. Santurkar, D. Tsipras, L. Engstrom, B. Tran, and A. Madry. Adversarial examples are not bugs, they are features. *NeurIPS*, 2019.
- [45] R. Geirhos, J.-H. Jacobsen, C. Michaelis, R. Zemel, W. Brendel, et al. Shortcut learning in deep neural networks. *Nature Machine Intelligence*, 2020.
- [46] R. A. Jacobs, M. I. Jordan, S. J. Nowlan, and G. E. Hinton. Adaptive mixtures of local experts. *Neural Computation*, 1991.
- [47] D. H. Wolpert. Stacked generalization. *Neural networks*, 1992.
- [48] A. Krogh and J. Vedelsby. Neural network ensembles, cross validation, and active learning. *NeurIPS*, 1994.
- [49] L. Breiman. Bagging predictors. *Machine learning*, 1996.
- [50] U. Johansson, C. Sönströd, U. Norinder, and H. Boström. Trade-off between accuracy and interpretability for predictive in silico modeling. *Future Medicinal Chemistry*, 2011.
- [51] G. Audemard, S. Bellart, L. Bounia, F. Koriche, J.-M. Lagniez, and P. Marquis. Trading complexity for sparsity in random forest explanations. In *AAAI*, 2022.
- [52] S. Bassan, G. Amir, M. Zehavi, and G. Katz. What makes an ensemble (un) interpretable? In *ICML*. PMLR, 2025.
- [53] F. Milletari, N. Navab, and S.-A. Ahmadi. V-net: Fully convolutional neural networks for volumetric medical image segmentation. In *3DV*. IEEE, 2016.
- [54] C. H. Sudre, W. Li, T. Vercauteren, S. Ourselin, and M. Jorge Cardoso. Generalised dice overlap as a deep learning loss function for highly unbalanced segmentations. In *DLMIA*. Springer, 2017.
- [55] Y. Lecun, L. Bottou, Y. Bengio, and P. Haffner. Gradient-based learning applied to document recognition. *Proceedings of the IEEE*, 1998.
- [56] J. Long, E. Shelhamer, and T. Darrell. Fully convolutional networks for semantic segmentation. In *CVPR*. IEEE, 2015.
- [57] D. Bonafilia, B. Tellman, T. Anderson, and E. Issenberg. Sen1floods11: A georeferenced dataset to train and test deep learning flood algorithms for sentinel-1. In *CVPR*. IEEE, 2020.
- [58] O. Ronneberger, P. Fischer, and T. Brox. U-net: Convolutional networks for biomedical image segmentation. In *MICCAI*. Springer, 2015.
- [59] J. Jakubik, S. Roy, C. E. Phillips, P. Fraccaro, D. Godwin, et al. Foundation models for generalist geospatial artificial intelligence. *arXiv*, 2023.
- [60] C. Gomes, B. Blumenstiel, J. L. d. S. Almeida, P. H. de Oliveira, P. Fraccaro, et al. Terratorch: The geospatial foundation models toolkit. *arXiv*, 2025.
- [61] T. Xiao, Y. Liu, B. Zhou, Y. Jiang, and J. Sun. Unified perceptual parsing for scene understanding. In *ECCV*. Springer, 2018.
- [62] N. Tajbakhsh, L. Jeyaseelan, Q. Li, J. N. Chiang, Z. Wu, and X. Ding. Embracing imperfect datasets: A review of deep learning solutions for medical image segmentation. *Medical Image Analysis*, 2020.
- [63] W. Shen, Z. Peng, X. Wang, H. Wang, J. Cen, et al. A survey on label-efficient deep image segmentation: Bridging the gap between weak supervision and dense prediction. *IEEE Pattern Analysis and Machine Intelligence*, 2023.
- [64] J. Quinonero-Candela, M. Sugiyama, A. Schwaighofer, and N. D. Lawrence. *Dataset Shift in Machine Learning*. MIT Press, 2008.
- [65] S. Ben-David, J. Blitzer, K. Crammer, A. Kulesza, F. Pereira, and J. W. Vaughan. A theory of learning from different domains. *Machine learning*, 2010.
- [66] C. Szegedy, W. Zaremba, I. Sutskever, J. Bruna, D. Erhan, et al. Intriguing properties of neural networks. In *ICLR*, 2014.
- [67] A. Madry, A. Makelov, L. Schmidt, D. Tsipras, and A. Vladu. Towards deep learning models resistant to adversarial attacks. In *ICLR*, 2018.
- [68] H. Zhang, M. Cisse, Y. N. Dauphin, and D. Lopez-Paz. mixup: Beyond empirical risk minimization. In *ICLR*, 2018.
- [69] S. Yun, D. Han, S. J. Oh, S. Chun, J. Choe, and Y. Yoo. Cutmix: Regularization strategy to train strong classifiers with localizable features. In *ICCV*. IEEE, 2019.
- [70] A. Paszke, S. Gross, F. Massa, A. Lerer, J. Bradbury, et al. Pytorch: An imperative style, high-performance deep learning library. *NeurIPS*, 2019.
- [71] D. P. Kingma and J. Ba. Adam: A method for stochastic optimization. *arXiv*, 2014.
- [72] I. Loshchilov and F. Hutter. Decoupled weight decay regularization. In *ICLR*, 2019.

